

POLYMER MODEL OF ZEOLITE THERMOCHEMICAL STABILITY

RANDOLPH ARTHUR^{1,*}, HIROSHI SASAMOTO², COLIN WALKER², AND MIKAZU YUI²

¹ INTERA, Inc., 3900 S. Wadsworth Blvd., Suite 555, Denver, Colorado, 80235, USA

² Japan Atomic Energy Agency, 4–33 Muramatsu, Tokai-mura, Naka-gun, Ibaraki-ken 319–1194, Japan

Abstract—The polymer model provides a relatively simple and robust basis for estimating the standard Gibbs free energies of formation (ΔG_f°) and standard enthalpies of formation (ΔH_f°) of clay minerals and other aluminosilicates with an accuracy that is comparable to or better than can be obtained using alternative techniques. The model developed in the present study for zeolites entailed the selection of internally consistent standard thermodynamic properties for model components, calibration of adjustable model parameters using a linear regression technique constrained by ΔG_f° and ΔH_f° values retrieved from calorimetric, solubility, and phase-equilibrium experiments, and assessments of model accuracy based on comparisons of predicted values with experimental counterparts not included in the calibration dataset. The ΔG_f° and ΔH_f° predictions were found to average within $\pm 0.2\%$ and $\pm 0.3\%$, respectively, of experimental values at 298.15 K and 1 bar. The latter result is comparable to the good accuracy that has been obtained by others using a more rigorous electronegativity-based model for ΔH_f° that accounts explicitly for differences in zeolite structure based on differences in framework density and unit-cell volume. This observation is consistent with recent calorimetric studies indicating that enthalpies of transition from quartz to various pure-silica zeolite frameworks (zeosils) are small and only weakly dependent on framework type, and suggests that the effects on ΔH_f° of differences in framework topology can be ignored for estimation purposes without incurring a significant loss of accuracy. The relative simplicity of the polymer model, together with its applicability to both zeolites and clay minerals, is based on a common set of experimentally determined and internally consistent thermodynamic properties for model components. These attributes are particularly well suited for studies of the effects of water-rock-barrier interactions on the long-term safety of geologic repositories for high-level nuclear waste (HLW).

Key Words—Estimation, Polymer Model, Standard Thermodynamic Properties, Zeolites.

INTRODUCTION

Widespread interest in the thermochemical stability of zeolites has resulted in the development of various empirical methods to estimate their standard thermodynamic properties (La Iglesia and Aznar, 1986; Chermak and Rimstidt, 1989; Mattigod and McGrail, 1999; Vieillard and Mathieu, 2009; Vieillard 2010; Mathieu and Vieillard, 2010). One such method, known as the polymer model, was revised in the present study.

The impetus for this work comes from international safety assessments of engineering concepts for the permanent disposal of nuclear wastes in deep geologic repositories (e.g. SKB, 2011). The assessments are based in part on predictions of how the geochemical environment within a repository might evolve over hundreds of thousands of years. In one evolution scenario, secondary zeolites, clay minerals, and other minerals in the CaO-Al₂O₃-SiO₂-H₂O (CASH) system are assumed to precipitate when cement-derived alkaline leachates (pH \geq 11) react with engineered barrier components (e.g. bentonite buffer, steel overpack, glass waste form) and

the host rock. Modeling studies have indicated that these secondary minerals can play an important role in controlling the geochemical environment and its spatial and temporal evolution (Savage *et al.*, 2002; Yui *et al.*, 2004; Oda *et al.*, 2004; Savage *et al.*, 2007).

Accounting for this role in a safety-assessment context is problematic, however, because zeolites (as well as some clay and CASH minerals) are complex solid solutions having variable compositions, and hence variable thermodynamic properties. A pragmatic approach to this problem is to assume as a first approximation that zeolites have a fixed stoichiometric composition selected from among many possible compositions that are in reality permitted by their variable chemistry. Alternative geochemical models in which different representative compositions for selected zeolites are assumed can then be used to generate a corresponding range of predicted geochemical environments for consideration in a safety assessment.

This bounding approach requires an ability to relate specific zeolite compositions to a corresponding set of standard thermodynamic properties that are needed to evaluate the geochemical models. Although these properties can be determined experimentally, a more practical approach is to estimate them using empirical methods given the large number of zeolite types and compositions that may be considered in a safety

* E-mail address of corresponding author:

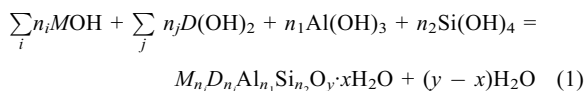
rarthur@intera.com

DOI: 10.1346/CCMN.2011.0590608

assessment. The objective of the present study was to revise the polymer model to ensure that it is internally consistent with respect to relevant thermodynamic databases, and can be used to reliably estimate ΔG_f° and ΔH_f° for zeolites of any specified composition. The basic polymer approach was considered in favor of alternative techniques because it can be used, in principle, with a single set of calorimetrically determined thermodynamic properties for model components to estimate ΔG_f° and ΔH_f° for zeolites, clay minerals (notably smectites and illites), and possibly other minerals in the CASH system, thereby providing an internally consistent basis for interpretation of the relative thermochemical stabilities of these closely associated phases. The supporting thermodynamic databases considered in this study (Yui *et al.*, 1999; Arthur *et al.* 1999) were developed by the Japan Atomic Energy Agency (JAEA) and are available online: <http://migrationdb.jaea.go.jp>.

BACKGROUND

The polymer model (Nriagu, 1975; Chen, 1975; Mattigod and Sposito, 1978; Sposito, 1985, 1986) was first applied to zeolites by Mattigod and McGrail (1999). These framework silicates were considered to be condensation copolymers of solid hydroxide components formed by the reaction:



where n_i represents the reaction coefficient for the i th monovalent exchangeable cation, M ; n_j denotes the reaction coefficient for the j th divalent exchangeable cation, D ; n_1 stands for the reaction coefficient for $Al(OH)_3$; n_2 refers to the reaction coefficient for $Si(OH)_4$, $y = (\sum n_i + 2\sum n_j + 3n_1 + 4n_2)/2$; and x represents the reaction coefficient for H_2O in extra-framework positions in the zeolite lattice.

The polymer model is based on the assumption that ΔG_f° for a zeolite of given composition can be closely

approximated by the reaction coefficient-weighted sum of ΔG_f° values for its hydroxide components plus a correction term, which accounts primarily for changes in the coordination environment of exchangeable cations as they are transferred from the components to exchange sites in the crystal lattice (Sposito, 1986). Similar corrections for tetrahedral cations (Si^{4+} and Al^{3+}) are assumed to be relatively small, which implies that ΔG_f° for the component of a tetrahedral cation in a solid hydroxide is similar to that for the same component in an aluminosilicate framework (Slaughter, 1966; Tardy and Garrels, 1974; Sposito, 1986). These constraints can be represented by the expression given in equation 2 (below) where the correction term is defined by adjustable parameters A (kJ mol^{-1}) and B ($\text{kJ mol}^{-1} \text{nm}^{-1}$) and by crystallographic ionic radii (nm) for monovalent, r_i , and divalent, r_j , exchangeable cations. The ΔG_f° values for components are assumed to be equal to those of the corresponding solid hydroxides or $H_2O_{(l)}$. The polymer model differs in this regard from alternative models in which oxide and/or hydroxide components are assumed to exist within the silicate (Tardy and Garrels, 1974, 1976; Chermak and Rimstidt, 1989).

The model's adjustable parameters can be determined by rearranging equation 2 to define a quantity, $\delta \Delta G_r^\circ$, given by equation 3 below. Using a calibration dataset of experimentally determined ΔG_f° values for zeolites, solid hydroxide components, and $H_2O_{(l)}$, the linear regression

of $\delta \Delta G_r^\circ$, as the dependent variable, *vs.* $\left(\sum_i n_i r_i + \sum_j n_j r_j \right)$, as the independent variable, can be used to determine the slope (B) and intercept (A) of equation 3.

Sposito (1985, 1986) considered the thermodynamic significance of parameter A in a polymer model for dioctahedral smectites. He noted that A can be interpreted as the standard Gibbs free energy of reaction (ΔG_r°) for the formation of a zero layer-charge phyllosilicate (pyrophyllite in this case) from component solid hydroxides. For zeolites, an analogous interpretation can be made by noting that the aluminosilicate framework,

$$\Delta G_{f,zeolite}^\circ = \sum_i n_i \Delta G_{f,MOH}^\circ + \sum_j n_j \Delta G_{f,D(OH)_2}^\circ + n_1 \Delta G_{f,Al(OH)_3}^\circ + n_2 \Delta G_{f,Si(OH)_4}^\circ - (y - x) \Delta G_{f,H_2O}^\circ - \left[A + B \left(\sum_i n_i r_i + \sum_j n_j r_j \right) \right] \quad (2)$$

$$\delta \Delta G_r^\circ = \Delta G_{f,zeolite}^\circ - \left(\sum_i n_i \Delta G_{f,MOH}^\circ + \sum_j n_j \Delta G_{f,D(OH)_2}^\circ + n_1 \Delta G_{f,Al(OH)_3}^\circ + n_2 \Delta G_{f,Si(OH)_4}^\circ - (y - x) \Delta G_{f,H_2O}^\circ \right) - \left[A + B \left(\sum_i n_i r_i + \sum_j n_j r_j \right) \right] \quad (3)$$

excluding hydrated exchangeable extra-framework cations and H_2O , has the general composition $[\text{Al}_{zm}\text{Si}_{(4-z)m}\text{O}_{8m}]^{zm-}$, where m stands for some multiple of this basic unit needed to fill the unit cell (Armbruster and Gunter, 2001). For the limiting case of zero net charge, $z = 0$, the framework composition is $\text{Si}_{4m}\text{O}_{8m}$, and formation of such a pure-silica zeolite from component $\text{Si}(\text{OH})_4$ can be represented by the general reaction $\text{Si}(\text{OH})_4 = \frac{1}{4m}\text{Si}_{4m}\text{O}_{8m} + 2\text{H}_2\text{O}_{(l)}$. Because free energy changes resulting from the transfer of a cation from an hydroxide component to a silicate framework are assumed to be relatively small in the polymer model, the constraint $\Delta G_r^0 = A = 0 \text{ kJ mol}^{-1}$ was assumed as a first approximation for any value of m in this reaction, and thus for all zeolites regardless of their composition. The validity of this assumption is evaluated further below. Mattigod and McGrail (1999) did not consider parameter A in their model, but presented an expression that is identical to equation 2 when $A = 0 \text{ kJ mol}^{-1}$.

Several other features of the Mattigod and McGrail (1999) model are pertinent to the present study. These investigators apparently used a ΔG_f^0 value for the amorphous hydrous oxide, $\text{SiO}_2 \cdot 2\text{H}_2\text{O}_{(\text{am})}$, to represent ΔG_f^0 for the stoichiometrically equivalent model component, $\text{Si}(\text{OH})_4$: this can be seen by noting that ΔG_r^0 for the dehydration reaction, $\text{SiO}_2 \cdot 2\text{H}_2\text{O}_{(\text{am})} = \text{SiO}_{2(\text{am})} + 2\text{H}_2\text{O}_{(l)}$, must equal 0 kJ mol^{-1} at any pressure and temperature if the conventional standard state calling for unit activity for pure solids and solvent $\text{H}_2\text{O}_{(l)}$ is assumed. As a result, $\Delta G_{f,\text{SiO}_2 \cdot 2\text{H}_2\text{O}_{(\text{am})}}^0 = \Delta G_{f,\text{SiO}_{2(\text{am})}}^0 + 2\Delta G_{f,\text{H}_2\text{O}_{(l)}}^0$, and, taking values for the two parameters on the right-hand side of this equation at 298.15 K and 1 bar from Wagman *et al.* (1982) ($-850.70 \text{ kJ mol}^{-1}$ and $-237.129 \text{ kJ mol}^{-1}$, respectively), gives $\Delta G_{f,\text{SiO}_2 \cdot 2\text{H}_2\text{O}_{(\text{am})}}^0 = -1324.96 \text{ kJ mol}^{-1}$. Mattigod and McGrail (1999) (with references to Wagman *et al.*, 1982) adopted a ΔG_f^0 value for $\text{Si}(\text{OH})_4 = -1324.9 \text{ kJ mol}^{-1}$, which differs significantly from the value given by Wagman *et al.* (1982) for the crystalline hydroxide, represented by $\text{H}_4\text{SiO}_{4(c)}$ ($-1332.9 \text{ kJ mol}^{-1}$). Thus, despite a minor difference in rounding, ΔG_f^0 for component $\text{Si}(\text{OH})_4$ in the Mattigod

and McGrail (1999) model apparently corresponds to that of the amorphous hydrous oxide, $\text{SiO}_2 \cdot 2\text{H}_2\text{O}_{(\text{am})}$. This observation is noteworthy because ΔG_f^0 values for all other components in this model [excluding $\text{H}_2\text{O}_{(l)}$] refer to the crystalline hydroxides.

Mattigod and McGrail (1999) assumed $B = 921 \text{ kJ mol}^{-1} \text{ nm}^{-1}$ based on the study of Sposito (1986), who evaluated this parameter using a model calibration dataset consisting of both estimated and experimental ΔG_f^0 values for 25 montmorillonites from Mattigod and Sposito (1978). Recalling that the correction term in the polymer model accounts for the effects on ΔG_f^0 of changes in the coordination of exchangeable cations as they are transferred from hydroxide components to exchange sites in a silicate lattice, the rationale for assuming that a B value for montmorillonites should necessarily also be appropriate for zeolites is unclear given that the structural frameworks of these two mineral groups differ significantly. Also noteworthy is the fact that Sposito (1986) determined $A = 41 \text{ kJ mol}^{-1}$ when $B = 921 \text{ kJ mol}^{-1} \text{ nm}^{-1}$, whereas Mattigod and McGrail (1999) effectively assumed $A = 0 \text{ kJ mol}^{-1}$.

Mattigod and McGrail (1999) did not extend their model for the purpose of estimating ΔH_f^0 , nor has the polymer model been used for such a purpose to the authors' knowledge. Most experimental investigations of the thermodynamic properties of zeolites have been based on direct calorimetric determinations of isobaric heat capacities and enthalpies of formation, however, and the results of these studies provide a valuable resource that can be used for model calibration and model testing. Because enthalpy, like Gibbs free energy, is a state function, such a model can be formulated in terms of the conceptual analogues of equations 2 and 3, given by equations 4 and 5 below, respectively, where A^* and B^* distinguish these adjustable parameters from their counterparts in equations 2 and 3. Consistent with the discussion concerning parameter A , the constraint $\Delta H_r^0 = A^* = 0 \text{ kJ mol}^{-1}$ was assumed as a first approximation for any value of m in the reaction $\text{Si}(\text{OH})_4 = \frac{1}{4m}\text{Si}_{4m}\text{O}_{8m} + 2\text{H}_2\text{O}_{(l)}$, and thus for all zeolites of any composition. The validity of this assumption is evaluated below.

$$\Delta H_{f,\text{zeolite}}^0 = \sum_i n_i \Delta H_{f,\text{MOH}}^0 + \sum_j n_j \Delta H_{f,\text{D}(\text{OH})_2}^0 + n_1 \Delta H_{f,\text{Al}(\text{OH})_3}^0 + n_2 \Delta H_{f,\text{Si}(\text{OH})_4}^0 - (y-x) \Delta H_{f,\text{H}_2\text{O}}^0 - \left[A^* + B^* \left(\sum_i n_i r_i + \sum_j n_j r_j \right) \right] \quad (4)$$

$$\delta \Delta H_r^0 = \Delta H_{f,\text{zeolite}}^0 - \left(\sum_i n_i \Delta H_{f,\text{MOH}}^0 + \sum_j n_j \Delta H_{f,\text{D}(\text{OH})_2}^0 + n_1 \Delta H_{f,\text{Al}(\text{OH})_3}^0 + n_2 \Delta H_{f,\text{Si}(\text{OH})_4}^0 - (y-x) \Delta H_{f,\text{H}_2\text{O}}^0 \right) - \left[A^* + B^* \left(\sum_i n_i r_i + \sum_j n_j r_j \right) \right] \quad (5)$$

MATERIALS AND METHODS

Revisions to the polymer model entailed the selection of thermodynamic properties for model components, calibration of parameters B and B^* using a linear regression technique and experimentally determined ΔG_f° and ΔH_f° values for zeolites reported in the literature up to and including 1999, and testing of the calibrated model by comparing model estimates with experimental values determined in studies carried out since 1999. This cut-off date was chosen because it resulted in roughly equivalent numbers of experimental studies supporting the calibration and testing datasets.

Selection of properties for model components

Most ΔG_f° and ΔH_f° values for model components were taken from Wagman *et al.* (1982) (Table 1). Corresponding values for $\text{H}_2\text{O}_{(l)}$, $\text{Al}(\text{OH})_{3(c)}$, and $\text{Mg}(\text{OH})_{2(c)}$ were selected from a different source (Arthur *et al.*, 1999) in order to maintain consistency with thermodynamic databases developed by JAEA. The ΔG_f° value for $\text{Sr}(\text{OH})_{2(c)}$ chosen by Mattigod and McGrail (1999) (referencing Robie *et al.*, 1978) was also used in the present study. Crystallographic ionic radii for exchangeable extra-framework cations were taken from Shannon (1976) (Table 2).

Component $\text{Si}(\text{OH})_4$ was represented in the model by the amorphous hydrous oxide $\text{SiO}_2 \cdot 2\text{H}_2\text{O}_{(\text{am})}$ following the approach of Mattigod and McGrail (1999). The corresponding ΔG_f° value (Table 1) was calculated based on recent solubility measurements for $\text{SiO}_2 \cdot n\text{H}_2\text{O}_{(\text{am})}$ (Gunnarsson and Arnórsson, 2000). The experimental results were interpreted in terms of the reaction $\text{SiO}_2 \cdot n\text{H}_2\text{O}_{(\text{am})} + 2\text{H}_2\text{O}_{(l)} = \text{H}_4\text{SiO}_{4(\text{aq})} + n\text{H}_2\text{O}_{(l)}$, for which the value of the equilibrium constant, K , is independent of hydration state, n (Gunnarsson and

Arnórsson, 2000). For $n = 2$, the reaction is $\text{SiO}_2 \cdot 2\text{H}_2\text{O}_{(\text{am})} = \text{H}_4\text{SiO}_{4(\text{aq})}$, and $\Delta G_r^\circ = \Delta G_{f,\text{H}_4\text{SiO}_4(\text{aq})}^\circ - \Delta G_{f,\text{SiO}_2 \cdot 2\text{H}_2\text{O}_{(\text{am})}}^\circ$. Rearranging this equation to $\Delta G_{f,\text{SiO}_2 \cdot 2\text{H}_2\text{O}_{(\text{am})}}^\circ = \Delta G_{f,\text{H}_4\text{SiO}_4(\text{aq})}^\circ - \Delta G_r^\circ$ and choosing values for the two parameters on the right-hand side ($-1309.181 \text{ kJ mol}^{-1}$ and $15.483 \text{ kJ mol}^{-1}$, respectively; Gunnarsson and Arnórsson, 2000) resulted in $\Delta G_{f,\text{SiO}_2 \cdot 2\text{H}_2\text{O}_{(\text{am})}}^\circ = -1324.66 \text{ kJ mol}^{-1}$. This value is slightly more positive than that adopted by Wagman *et al.* (1982) and Mattigod and McGrail (1999). The $\Delta G_{f,\text{H}_4\text{SiO}_4(\text{aq})}^\circ$ value used in this analysis is compatible with recent quartz solubility measurements at low temperatures (Rimstidt 1997). The ΔH_f° value for component $\text{Si}(\text{OH})_4$ was calculated based on the above reaction using ΔH_r° and $\Delta H_{f,\text{H}_4\text{SiO}_4(\text{aq})}^\circ$ values at 298.15 K and 1 bar ($14.595 \text{ kJ mol}^{-1}$ and $-1461.722 \text{ kJ mol}^{-1}$, respectively) from Gunnarsson and Arnórsson (2000).

Calibration datasets

The regression procedure was constrained by 23 ΔG_f° values for various zeolites derived from calorimetric, phase-equilibrium, and solubility studies (Table 3). The calorimetric values were calculated in the referenced studies using ΔH_f° and standard entropies (S°) retrieved from high-temperature lead-borate calorimetry or from heats of solution measured at low temperatures in hydrofluoric acid (HF) solutions. Calorimetric ΔG_f° values from compilations in which the corresponding standard entropies were either estimated or taken from other literature sources were not included in the regression dataset. Phase-equilibrium and solubility study values were included in the regression dataset because they were considered to be at least as reliable as their calorimetric counterparts (Helgeson *et al.*, 1978; Nordstrom *et al.*, 1990). The ΔG_f° values retrieved from solubilities measured by Wilkin and Barnes (1998) for Na- and K-exchanged variants of a natural clinoptilolite from Castle Creek, Idaho, for example, are closely consistent with calorimetric ΔH_f° and S° values determined for these minerals by Yang *et al.* (2001).

Values of ΔH_f° for 63 hydrated zeolites were used in the regression procedure to determine B^* (Table 4). This dataset features a diverse set of zeolite types having a

Table 1. ΔG_f° and ΔH_f° values for model components.

Compound	ΔG_f° (kJ mol ⁻¹)	ΔH_f° (kJ mol ⁻¹)
$\text{H}_2\text{O}_{(l)}$	-237.18 ^a	-285.84 ^a
$\text{Al}(\text{OH})_{3(c)}$	-1154.89 ^a	-1293.13 ^a
$\text{Ba}(\text{OH})_{2(c)}$	-859.5 ^b	-944.7 ^c
$\text{Ca}(\text{OH})_{2(c)}$	-898.49 ^c	-986.09 ^c
$\text{KOH}_{(c)}$	-379.08 ^c	-424.764 ^c
$\text{LiOH}_{(c)}$	-438.95 ^c	-484.93 ^c
$\text{Mg}(\text{OH})_{2(c)}$	-835.32 ^a	-926.3 ^a
$\text{NaOH}_{(c)}$	-379.494 ^c	-425.609 ^c
$\text{RbOH}_{(c)}$	-364.4 ^d	-418.19 ^c
$\text{Si}(\text{OH})_4$ ($\text{SiO}_2 \cdot 2\text{H}_2\text{O}_{(\text{am})}$)	-1324.66 ^e	-1476.32 ^e
$\text{Sr}(\text{OH})_{2(c)}$	-881.1 ^f	-959.0 ^f

^a JAEA TDB 990900 (Arthur *et al.*, 1999); ^b JANAF (Stull and Prophet, 1971); ^c Wagman *et al.* (1982); ^d Mattigod and Sposito (1978); ^e Gunnarsson and Arnórsson (2000);

^f Mattigod and McGrail (1999)

(c) crystalline; (am) amorphous.

Table 2. Crystallographic ionic radii (Shannon, 1976).

Cation	Radius (nm)
Ba^{2+}	0.135
Ca^{2+}	0.100
K^+	0.138
Li^+	0.076
Mg^{2+}	0.072
Na^+	0.102
Rb^+	0.152
Sr^{2+}	0.118

Table 3. Calibration dataset of experimental ΔG_f° values at 298.15 K and 1 bar.

Zeolite	Composition	ΔG_f° (kJ mol ⁻¹)	Basis*	Ref.**
Analcime	Na ₂ Al ₂ Si ₄ O ₁₂ ·2H ₂ O	-6176.4	<i>p</i>	1
Analcime	Na _{1.92} Al _{1.92} Si _{4.08} O ₁₂ ·2H ₂ O	-6172.2	<i>c</i>	2
Heulandite	Ba _{0.065} Sr _{0.175} Na _{0.383} Ca _{0.585} K _{0.132} Al _{2.165} Si _{6.835} O ₁₈ ·6H ₂ O	-9807.0	<i>c</i>	2
Mesolite	Na _{0.676} Ca _{0.657} Al _{1.99} Si _{3.01} O ₁₀ ·2.647H ₂ O	-5527.3	<i>c</i>	2
Mordenite	Ca _{0.578} Na _{0.722} Al _{1.88} Si _{10.12} O ₂₄ ·6.936H ₂ O	-12495.2	<i>c</i>	2
Natrolite	Na ₂ Al ₂ Si ₃ O ₁₀ ·2H ₂ O	-5330.7	<i>c</i>	2
Scolecite	CaAl ₂ Si ₃ O ₁₀ ·3H ₂ O	-5612.0	<i>c</i>	2
Leonhardtite	CaAl ₂ Si ₄ O ₁₂ ·3.5H ₂ O	-6583.4	<i>c</i>	3
Merlinoite	K ₂ Al ₂ Si _{3.88} O _{11.76} ·3.38H ₂ O	-6482.8	<i>c</i>	3
Merlinoite	K ₂ Al ₂ Si _{3.62} O _{11.24} ·3.38H ₂ O	-6246.6	<i>c</i>	3
Merlinoite	K _{1.6} Na _{0.4} Al ₂ Si _{3.88} O _{11.76} ·3.62H ₂ O	-6544.4	<i>c</i>	3
Merlinoite	K _{1.82} Na _{0.18} Al ₂ Si _{3.62} O _{11.24} ·3.58H ₂ O	-6289.2	<i>c</i>	3
Merlinoite	K _{0.38} Na _{1.62} Al ₂ Si _{3.88} O _{11.76} ·4.26H ₂ O	-6651.6	<i>c</i>	3
Merlinoite	K _{0.38} Na _{1.62} Al ₂ Si _{3.62} O _{11.24} ·4.36H ₂ O	-6450.6	<i>c</i>	3
Yugawaralite	CaAl ₂ Si ₆ O ₁₆ ·4H ₂ O	-8387.7	<i>p</i>	4
Heulandite	CaAl ₂ Si ₇ O ₁₈ ·6H ₂ O	-9722.3	<i>p</i>	5
Analcime	NaAlSi ₂ O ₆ ·H ₂ O	-3089.1 ^a	<i>s</i>	6
Analcime	Na _{0.85} Al _{0.85} Si _{2.15} O ₆ ·H ₂ O	-3043.9 ^a	<i>s</i>	6
Na-clinoptilolite	Na _{1.1} Al _{1.1} Si _{4.9} O ₁₂ ·3.5H ₂ O	-6267.7 ^a	<i>s</i>	6
K-clinoptilolite	K _{1.1} Al _{1.1} Si _{4.9} O ₁₂ ·2.7H ₂ O	-6109.7 ^a	<i>s</i>	6
Analcime	Na _{1.02} Al _{1.02} Si _{1.98} O ₆ ·H ₂ O	-3090.5 ^a	<i>s</i>	7
Na-clinoptilolite	Na ₂ Al ₂ Si ₁₀ O ₂₄ ·8H ₂ O	-12717.5 ^a	<i>s</i>	7
Stilbite	Ca _{1.019} Na _{0.136} K _{0.006} Al _{2.18} Si _{6.82} O ₁₈ ·7.33H ₂ O	-10142.0	<i>c</i>	8

* Experimental basis : *p* – phase equilibrium, *c* – calorimetry, *s* – solubility.

** Reference: 1 – Helgeson *et al.* (1978); 2 – Johnson *et al.* (1992a); 3 – Donahoe *et al.* (1990a); 4 – Zeng and Liou (1982); 5 – Cho *et al.* (1987); 6 – Wilkin and Barnes (1998); 7 – Murphy *et al.* (1996); 8 – Howell *et al.* (1990).

^a Recalculated using experimental solubilities and standard partial molal Gibbs free energies of formation of aqueous reactant and product species from JAEA TDB 990900 (Arthur *et al.*, 1999).

wide range of Al/Si ratios and extra-framework compositions. All of the calorimetric values were also included in a recent critical compilation of reliable ΔH_f° data for anhydrous and hydrated zeolites (Mathieu and Vieillard, 2010). Reported ΔH_f° from the constituent oxides were converted in the present study to ΔH_f° from the elements using auxiliary data from Wagman *et al.* (1982) for ΔH_f° of the oxides from the elements. A large number of ΔH_f° values for synthetic anhydrous zeolites, for which hydration enthalpies have also been determined by transposed-temperature drop calorimetry, were not included in the calibration dataset either because the respective chemical formulae were not perfectly balanced or because interpretations of the structural chemistry of constituent ions (notably Al) were complicated by possible interstratifications within these compounds (Mathieu and Vieillard, 2010).

Regression procedure

A linear regression technique was used with the calibration datasets to determine model parameters *B* and *B**, respectively. The regression procedure entailed calculation of the quantity $\delta\Delta G_r^\circ$ using reaction coefficients n_i , n_j , n_1 , n_2 , and $(y-x)$ and experimental ΔG_f° values for the zeolites (Table 3) and their respective

components (Table 1). Calculations of the quantity $\delta\Delta H_r^\circ$ were carried out using a similar procedure constrained by experimental ΔH_f° values for the zeolites (Table 4) and components (Table 1). The quantity $\left(\sum_i n_i r_i + \sum_j n_j r_j\right)$ was calculated using reaction coefficients for the exchangeable cations and their respective ionic radii (Table 2). Parameter *B* was determined by linear regression of $\delta\Delta G_r^\circ$ and corresponding $\left(\sum_i n_i r_i + \sum_j n_j r_j\right)$ values with the constraint *A* = 0 kJ mol⁻¹. Parameter *B** was determined similarly using the $\delta\Delta H_r^\circ$ and $\left(\sum_i n_i r_i + \sum_j n_j r_j\right)$ data with *A** = 0 kJ mol⁻¹.

RESULTS

The regression procedure was used to determine *B* = 966±43 kJ mol⁻¹ nm⁻¹ (Figure 1) and *B** = 684±42 kJ mol⁻¹ nm⁻¹ (Figure 2). This *B* value for zeolites is identical, within uncertainty limits, to that determined by Sposito (1986) for dioctahedral smectites (*B* = 921±108 kJ mol⁻¹ nm⁻¹). The effects on ΔG_f° of changes in the coordination environment of exchangeable cations as they are transferred from hydroxide components to

Table 4. Calibration dataset of experimental ΔH_f° values (kJ mol⁻¹) at 298.15 K and 1 bar.

Zeolite	Composition	ΔH_f°	Basis*	Ref.**
Analcime	Na ₂ Al ₂ Si ₄ O ₁₂ ·2H ₂ O	-6612.3	<i>p</i>	1
Analcime	Na _{1.92} Al _{1.92} Si _{4.08} O ₁₂ ·2H ₂ O	-6611.6	<i>c</i>	2
Heulandite	Ba _{0.065} Sr _{0.175} Na _{0.383} Ca _{0.585} K _{0.132} Al _{2.165} Si _{6.835} O ₁₈ ·6H ₂ O	-10622.5	<i>c</i>	2
Mesolite	Na _{0.676} Ca _{0.657} Al _{1.99} Si _{3.01} O ₁₀ ·2.647H ₂ O	-5961.2	<i>c</i>	2
Mordenite	Ca _{0.578} Na _{0.722} Al _{1.88} Si _{10.12} O ₂₄ ·6.936H ₂ O	-13512.4	<i>c</i>	2
Natrolite	Na ₂ Al ₂ Si ₃ O ₁₀ ·2H ₂ O	-5732.7	<i>c</i>	2
Scolecite	CaAl ₂ Si ₃ O ₁₀ ·3H ₂ O	-6063.1	<i>c</i>	2
Laumontite	CaAl ₂ Si ₄ O ₁₂ ·4H ₂ O	-7251.0	<i>c</i>	3
Wairakite	CaAl ₂ Si ₄ O ₁₂ ·2H ₂ O	-6646.7	<i>c</i>	3
Yugawaralite	CaAl ₂ Si ₆ O ₁₆ ·4H ₂ O	-9051.3	<i>c</i>	3
Leonhardite	CaAl ₂ Si ₄ O ₁₂ ·3.5H ₂ O	-7107.3	<i>c</i>	3,4
Ca-leonhardite	CaAl ₂ Si ₄ O ₁₂ ·3.65H ₂ O	-7154.5	<i>c</i>	4
Na-leonhardite	Na _{1.5} K _{0.05} Ca _{0.2} Al ₂ Si ₄ O _{11.975} ·2.8H ₂ O	-6799.1	<i>c</i>	4
K-leonhardite	Na _{0.05} K _{1.05} Ca _{0.55} Al ₂ Si _{3.95} O ₁₂ ·1.3H ₂ O	-6466.6	<i>c</i>	4
Primary leonhardite	Na _{0.3} K _{0.4} Ca _{0.65} Al ₂ Si ₄ O ₁₂ ·3.5H ₂ O	-7126.9	<i>c</i>	4
Merlinoite	K ₂ Al ₂ Si _{3.88} O _{11.76} ·3.38H ₂ O	-6963.6	<i>c</i>	5
Merlinoite	K ₂ Al ₂ Si _{3.62} O _{11.24} ·3.38H ₂ O	-6720.0	<i>c</i>	5
Merlinoite	K _{1.6} Na _{0.4} Al ₂ Si _{3.88} O _{11.76} ·3.62H ₂ O	-7038.0	<i>c</i>	5
Merlinoite	K _{1.82} Na _{0.18} Al ₂ Si _{3.62} O _{11.24} ·3.58H ₂ O	-6774.6	<i>c</i>	5
Merlinoite	K _{0.38} Na _{1.62} Al ₂ Si _{3.88} O _{11.76} ·4.26H ₂ O	-7182.4	<i>c</i>	5
Merlinoite	K _{0.38} Na _{1.62} Al ₂ Si _{3.62} O _{11.24} ·4.36H ₂ O	-6976.6	<i>c</i>	5
Yugawaralite	CaAl ₂ Si ₆ O ₁₆ ·4H ₂ O	-9036.2	<i>p</i>	6
Natrolite	Na ₂ Al ₂ Si ₃ O ₁₀ ·2H ₂ O	-5769.9	<i>c</i>	7
Tetranatrolite	Na ₂ Al ₂ Si ₃ O ₁₀ ·2H ₂ O	-5743.7	<i>c</i>	7
Scolecite	CaAl ₂ Si ₃ O ₁₀ ·3H ₂ O	-6100.7	<i>c</i>	7
Mesolite	Na ₂ Ca ₂ Al ₆ Si ₉ O ₃₀ ·8H ₂ O	-17943.9	<i>c</i>	7
Thomsonite	NaCa ₂ Al ₃ Si ₅ O ₂₀ ·6H ₂ O	-12464.8	<i>c</i>	7
Gonnardite	Na _{0.16} Ca _{1.95} Al ₄ Si ₆ O ₂₀ ·6H ₂ O	-12198.6	<i>c</i>	7
Edingtonite	Ba _{0.97} K _{0.03} Na _{0.04} Al _{1.98} Si _{3.01} O _{9.995} ·4H ₂ O	-6376.0	<i>c</i>	7
Stillbite	Ca _{1.019} Na _{0.136} K _{0.006} Al _{2.18} Si _{6.82} O ₁₈ ·7.33H ₂ O	-11033.6	<i>c</i>	8
Heulandite	CaAl ₂ Si ₇ O ₁₈ ·6H ₂ O	-10524.3	<i>p</i>	9
Bikitaite	Li ₂ Al ₂ Si ₄ O ₁₂ ·2H ₂ O	-6718.8	<i>c</i>	10
Chabazite	Ca _{1.58} K _{0.36} Al _{3.34} Si _{8.66} O _{24.09} ·12.83H ₂ O	-15691.8	<i>c</i>	11
Chabazite	Ca _{2.24} K _{0.52} Al _{4.91} Si _{7.09} O _{24.045} ·14.68H ₂ O	-16674.9	<i>c</i>	11
Chabazite	Ca _{2.29} K _{0.04} Na _{0.04} Al _{4.07} Si _{7.93} O _{24.295} ·13.4H ₂ O	-16281.2	<i>c</i>	11
Chabazite	Sr _{0.08} Ca _{2.8} K _{0.06} Al _{4.8} Si _{7.2} O _{24.51} ·12.95H ₂ O	-16529.3	<i>c</i>	11
Chabazite	Ca _{2.84} Al _{4.71} Si _{7.29} O _{24.485} ·15.16H ₂ O	-17150.4	<i>c</i>	11
Chabazite	K _{3.23} Al _{3.31} Si _{8.69} O _{23.96} ·8.9H ₂ O	-14529.4	<i>c</i>	11
Chabazite	K _{3.39} Al _{3.18} Si _{8.82} O _{24.105} ·9.88H ₂ O	-14870.3	<i>c</i>	11
Chabazite	K _{4.79} Al _{4.89} Si _{7.11} O _{23.95} ·10.63H ₂ O	-15439.4	<i>c</i>	11
Chabazite	K _{5.39} Al _{5.87} Si _{6.13} O _{23.76} ·10.71H ₂ O	-15641.3	<i>c</i>	11
Chabazite	Li _{3.05} K _{0.01} Na _{0.13} Al _{3.25} Si _{8.75} O _{23.97} ·11.79H ₂ O	-15379.7	<i>c</i>	11
Chabazite	Li _{3.17} K _{0.01} Na _{0.15} Al _{3.32} Si _{8.68} O _{24.005} ·10.88H ₂ O	-15145.2	<i>c</i>	11
Chabazite	Sr _{0.17} Li _{3.75} K _{0.02} Na _{0.15} Al _{4.89} Si _{7.11} O _{23.685} ·12.52H ₂ O	-15929.2	<i>c</i>	11
Chabazite	Li _{3.27} K _{0.02} Na _{0.62} Al _{3.96} Si _{8.04} O _{23.975} ·12.59H ₂ O	-15868.2	<i>c</i>	11
Chabazite	Li _{3.76} K _{0.01} Na _{0.2} Al _{4.04} Si _{7.96} O _{23.965} ·12.7H ₂ O	-15895.1	<i>c</i>	11
Chabazite	Li _{4.7} K _{0.01} Na _{0.24} Al _{4.96} Si _{7.04} O _{23.995} ·14.52H ₂ O	-16608.5	<i>c</i>	11
Chabazite	Li _{5.6} Na _{0.02} Al _{5.75} Si _{6.25} O _{23.935} ·15.17H ₂ O	-17097.6	<i>c</i>	11
Chabazite	K _{0.01} Na _{3.33} Al _{3.31} Si _{8.69} O _{24.015} ·11.69H ₂ O	-15235.5	<i>c</i>	11
Chabazite	K _{0.01} Na _{3.95} Al ₄ Si ₈ O _{23.98} ·12.57H ₂ O	-15717.1	<i>c</i>	11
Chabazite	K _{0.02} Na _{4.28} Al _{3.98} Si _{8.02} O _{24.16} ·11.89H ₂ O	-15663.2	<i>c</i>	11
Chabazite	Ca _{0.02} K _{0.01} Na _{5.51} Al _{5.85} Si _{6.15} O _{23.855} ·16.5H ₂ O	-17130.3	<i>c</i>	11
Chabazite	Ca _{1.63} K _{0.13} Na _{0.03} Al _{3.23} Si _{8.77} O _{24.095} ·12.54H ₂ O	-15652.2	<i>c</i>	11
Clinoptilolite	Ca _{0.53} Mg _{0.08} K _{0.25} Na _{0.08} Al _{1.61} Si _{7.39} O ₁₈ ·5.56H ₂ O	-10306.1	<i>c</i>	12
Heulandite	Sr _{0.1} Ca _{0.75} K _{0.04} Na _{0.41} Al _{2.28} Si _{6.75} O _{18.001} ·6.11H ₂ O	-10770.4	<i>c</i>	12
Edingtonite	Ba _{1.93} K _{0.08} Na _{0.06} Al _{3.96} Si _{6.03} O ₂₀ ·7.38H ₂ O	-12583.8	<i>c</i>	13
Thomsonite	Ca _{8.16} Na _{3.52} Al ₂₀ Si _{20.12} O _{80.22} ·25.36H ₂ O	-50305.8	<i>c</i>	13
Analcime	Na _{0.96} Al _{0.96} Si _{2.04} O ₆ ·H ₂ O	-3305.8	<i>c</i>	14
Heulandite	Ba _{0.065} Sr _{0.175} Ca _{0.585} K _{0.132} Al _{2.165} Si _{6.835} O ₁₈ ·6H ₂ O	-10594.6	<i>c</i>	15
Mesolite	Ca _{0.657} Na _{0.676} Al _{1.99} Si _{3.01} O ₁₀ ·2.647H ₂ O	-5961.2	<i>c</i>	16
Natrolite	Na ₂ Al ₂ Si ₃ O ₁₀ ·2H ₂ O	-5732.7	<i>c</i>	16
Scolecite	CaAl ₂ Si ₃ O ₁₀ ·3H ₂ O	-6063.1	<i>c</i>	16
Analcime	K _{0.01375} Na _{0.9825} Al _{0.9375} Si _{2.0475} O ₆ ·H ₂ O	-3280.7	<i>c</i>	17

* Experimental basis : *p* – phase equilibrium, *c* – calorimetry.** Reference : 1 – Helgeson *et al.* (1978); 2 – Johnson *et al.* (1992a); 3 – Kiseleva *et al.* (1996a); 4 – Kiseleva *et al.* (1996b); 5 – Donahoe *et al.* (1990b); 6 – Zeng and Liou (1982); 7 – Kiseleva *et al.* (1997); 8 – Howell *et al.* (1990); 9 – Cho *et al.* (1987); 10 – Mel'chakova *et al.* (1999); 11 – Shim *et al.* (1999); 12 – Petrova (1997); 13 – Kiseleva *et al.* (1998); 14 – Johnson *et al.* (1982); 15 – Johnson *et al.* (1985); 16 – Johnson *et al.* (1983); 17 – Ogorodova *et al.* (1996).

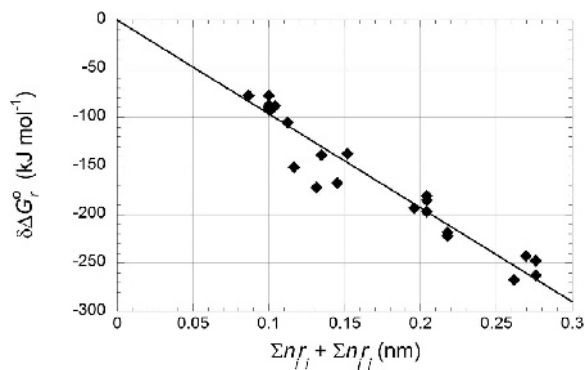


Figure 1. Plot of $\delta\Delta G_f^0$ vs. $(\Sigma n_i r_i + \Sigma n_j r_j)$. The value of $-B$ is given by the slope of the best-fit line through the data (-966 ± 43 $\text{kJ mol}^{-1} \text{nm}^{-1}$). Uncertainty limits correspond to the 95% confidence level. $R^2 = 0.9247$.

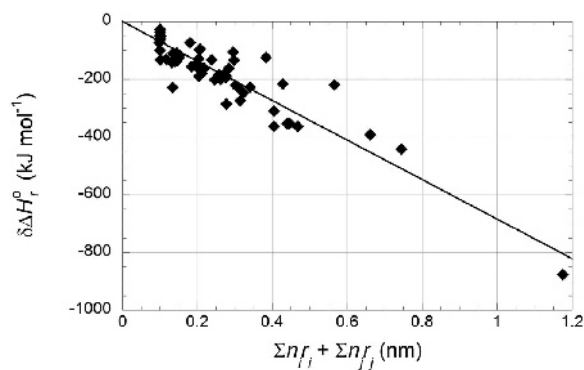


Figure 2. Plot of $\delta\Delta H_f^0$ vs. $(\Sigma n_i r_i + \Sigma n_j r_j)$. The value of $-B^*$ is given by the slope of the best-fit line through the data (-684 ± 42 $\text{kJ mol}^{-1} \text{nm}^{-1}$). Uncertainty limits correspond to the 95% confidence level. $R^2 = 0.8419$.

exchange sites in a silicate lattice are thus apparently similar for zeolites and montmorillonites, and possibly other 2:1 layer-type phyllosilicates.

The accuracy of the calibrated model was assessed by comparing predictions of ΔG_f^0 and ΔH_f^0 values for specific zeolite compositions with their experimental counterparts determined in studies carried out since 1999. Differences between predicted and experimental ΔG_f^0 values were small, averaging within $\sim\pm 0.20\%$ for 16 zeolites (Table 5). Differences between estimated and experimental ΔH_f^0 values were also small, averaging within $\sim\pm 0.30\%$ for 33 zeolites (Table 6).

Uncertainties in the ΔG_f^0 and ΔH_f^0 estimates were difficult to quantify. Standard errors were strongly correlated in the regression procedure and, therefore, do not provide a reliable basis for quantifying the uncertainty in estimates for minerals outside the calibration dataset. The number of minerals in this dataset was, moreover, relatively small compared to the number of regression components. Given these limitations, no attempt was made to refine the regression procedure by taking into account experimental uncertainties in ΔG_f^0 and ΔH_f^0 values for model components and zeolites. A guide to the overall uncertainty

Table 5. Comparison of experimental (Exp.) and estimated (Est.) ΔG_f^0 values at 298.15 K and 1 bar.

Zeolite	Composition	$-\Delta G_f^0$ (kJ mol^{-1})		Diff. (%)**
		Exp.	Est.	
Stilbite	$\text{Ca}_2\text{NaAl}_5\text{Si}_{13}\text{O}_{36}\cdot 16\text{H}_2\text{O}$	-20696.1 ^a	-20719.5	-0.11
Stellerite	$\text{Ca}_2\text{Al}_4\text{Si}_{14}\text{O}_{36}\cdot 14\text{H}_2\text{O}$	-19924.4 ^a	-19936.9	-0.06
Clinoptilolite	$\text{Ca}_{0.56}\text{Al}_{1.12}\text{Si}_{4.88}\text{O}_{12}\cdot 3.9\text{H}_2\text{O}$	-6386.3 ^{b,*}	-6393.9	-0.12
Mordenite	$\text{Ca}_{0.515}\text{Al}_{1.03}\text{Si}_{4.97}\text{O}_{12}\cdot 3.1\text{H}_2\text{O}$	-6162.7 ^{b,*}	-6174.7	-0.19
Clinoptilolite	$\text{Na}_{0.085}\text{K}_{0.037}\text{Ca}_{0.01}\text{Mg}_{0.02}\text{Al}_{0.182}\text{Si}_{0.818}\text{O}_2\cdot 0.528\text{H}_2\text{O}$	-1034.01 ^c	-1032.3	0.17
Clinoptilolite	$\text{Ca}_{0.084}\text{Mg}_{0.008}\text{Al}_{0.182}\text{Si}_{0.818}\text{O}_2\cdot 0.646\text{H}_2\text{O}$	-1064.95 ^c	-1063.4	0.14
Clinoptilolite	$\text{Na}_{0.182}\text{Al}_{0.182}\text{Si}_{0.818}\text{O}_2\cdot 0.572\text{H}_2\text{O}$	-1044.19 ^c	-1042.1	0.20
Clinoptilolite	$\text{K}_{0.182}\text{Al}_{0.182}\text{Si}_{0.818}\text{O}_2\cdot 0.433\text{H}_2\text{O}$	-1014.89 ^c	-1015.4	-0.04
Clinoptilolite	$\text{Na}_{0.097}\text{K}_{0.085}\text{Al}_{0.182}\text{Si}_{0.818}\text{O}_2\cdot 0.495\text{H}_2\text{O}$	-1027.26 ^c	-1026.7	0.05
Heulandite	$\text{Ca}_{0.86}\text{Na}_{0.37}\text{K}_{0.06}\text{Al}_{2.14}\text{Si}_{6.86}\text{O}_{18}\cdot 6.1\text{H}_2\text{O}$	-9835.7 ^d	-9799.5	0.37
Stilbite	$\text{Ca}_{1.01}\text{Na}_{0.12}\text{Al}_{2.12}\text{Si}_{6.88}\text{O}_{18}\cdot 7.27\text{H}_2\text{O}$	-10130.9 ^d	-10079.4	0.51
Chabazite	$\text{Ca}_{1.65}\text{Na}_{0.24}\text{K}_{0.1}\text{Al}_{3.79}\text{Si}_{8.25}\text{O}_{24}\cdot 12.47\text{H}_2\text{O}$	-14365.9 ^e	-14378.6	-0.09
Chabazite	$\text{K}_{1.96}\text{Na}_{0.34}\text{Ca}_{1.02}\text{Sr}_{0.03}\text{Ba}_{0.01}\text{Al}_{3.96}\text{Si}_{7.92}\text{O}_{24}\cdot 12.73\text{H}_2\text{O}$	-14549.0 ^e	-14613.0	-0.44
Analcime	$\text{Na}_{1.05}\text{Al}_{1.05}\text{Si}_{1.95}\text{O}_6\cdot 0.975\text{H}_2\text{O}$	-3097.96 ^f	-3105.8	-0.25
Analcime	$\text{Na}_{0.75}\text{Al}_{0.75}\text{Si}_{2.25}\text{O}_6\cdot 1.125\text{H}_2\text{O}$	-3044.46 ^f	-3048.9	-0.15
Analcime	$\text{Na}_{1.05}\text{Al}_{1.05}\text{Si}_{1.95}\text{O}_6\cdot 0.975\text{H}_2\text{O}$	-3097.0 ^g	-3105.8	-0.28
Mean absolute value				0.20

^a Fridriksson *et al.* (2001); ^b Benning *et al.* (2000); ^c Yang *et al.* (2001); ^d Kiseleva *et al.* (2001a); ^e Ogorodova *et al.* (2002a); ^f Neuhoff *et al.* (2004); ^g Redkin and Hemley (2000).

* recalculated using experimental solubility data and standard partial molal Gibbs free energies of formation of aqueous reactant and product species from JAEA TDB 990900 (Arthur *et al.*, 1999).

** Diff. = $[(\text{experimental } \Delta G_f^0 - \text{estimated } \Delta G_f^0) / \text{estimated } \Delta G_f^0] \times 100$

Table 6. Comparison of experimental (Exp.) and estimated (Est.) ΔH_f^0 values at 298.15 K and 1 bar.

Zeolite	Composition	ΔH_f^0 (kJ mol ⁻¹)		– Diff. (%)* –	
		Exp.	Est.	Present study	M&V**
Stilbite	Ca ₂ NaAl ₅ Si ₁₃ O ₃₆ ·16H ₂ O	–22579.7 ¹	–22545.4	0.15	–
Stellerite	Ca ₂ Al ₄ Si ₁₄ O ₃₆ ·14H ₂ O	–21656.2 ¹	–21661.5	–0.03	–
Clinoptilolite	Na _{0.085} K _{0.037} Ca _{0.01} Mg _{0.02} Al _{0.182} Si _{0.818} O ₂ ·0.528H ₂ O	–1117.57 ²	–1113.6	0.36	0.67
Clinoptilolite	Ca _{0.084} Mg _{0.008} Al _{0.182} Si _{0.818} O ₂ ·0.646H ₂ O	–1153.78 ²	–1152.3	0.13	–0.13
Clinoptilolite	Na _{0.182} Al _{0.182} Si _{0.818} O ₂ ·0.572H ₂ O	–1130.05 ²	–1125.0	0.45	0.21
Clinoptilolite	K _{0.182} Al _{0.182} Si _{0.818} O ₂ ·0.433H ₂ O	–1094.21 ²	–1089.6	0.43	0.44
Clinoptilolite	Na _{0.097} K _{0.085} Al _{0.182} Si _{0.818} O ₂ ·0.495H ₂ O	–1109.49 ²	–1105.0	0.41	0.28
Heulandite	Ca _{0.86} Na _{0.37} K _{0.06} Al _{2.14} Si _{6.86} O ₁₈ ·6.1H ₂ O	–10656.3 ³	–10614.7	0.39	–0.23
Stilbite	Ca _{1.01} Na _{0.12} Al _{2.12} Si _{6.88} O ₁₈ ·7.27H ₂ O	–11017.9 ³	–10956.0	0.56	0.14
Chabazite	Ca _{1.65} Na _{0.24} K _{0.1} Al _{3.79} Si _{8.25} O ₂₄ ·12.47H ₂ O	–15715.7 ⁴	–15695.6	0.13	0.07
Chabazite	K _{1.96} Na _{0.34} Ca _{1.02} Sr _{0.03} Ba _{0.01} Al _{3.96} Si _{7.92} O ₂₄ ·12.73H ₂ O	–15924.0 ⁴	–15895.0	0.18	0.23
Stellerite	Ca _{1.02} Al _{2.01} Si _{6.98} O ₁₈ ·7.04H ₂ O	–10909.1 ⁵	–10846.7	0.57	0.02
Analcime	Na _{1.05} Al _{1.05} Si _{1.95} O ₆ ·0.975H ₂ O	–3317.28 ⁶	–3320.4	–0.10	–
Analcime	Na _{0.75} Al _{0.75} Si _{2.25} O ₆ ·1.125H ₂ O	–3264.29 ⁶	–3269.6	–0.16	–
Analcime	Na _{1.05} Al _{1.05} Si _{1.95} O ₆ ·0.975H ₂ O	–3316.3 ⁷	–3320.4	–0.13	–
Amichite	Ca _{0.22} K _{3.84} Na _{3.88} Al _{8.06} Si _{7.9} O _{32.03} ·9.86H ₂ O	–19906.7 ⁸	–19896.3	0.05	0.35
Brewsterite	Ba _{0.66} Sr _{1.3} K _{0.02} Na _{0.06} Al ₄ Si ₁₂ O ₃₂ ·10.1H ₂ O	–19004.3 ⁹	–18704.7	1.58	0.22
Dachiardite	Ca _{0.66} Mg _{0.1} K _{0.35} Na _{2.21} Al _{4.41} Si _{19.67} O _{47.99} ·11.8H ₂ O	–26592.9 ¹⁰	–26467.4	0.47	0.44
Erionite	Ca _{2.06} Mg _{1.18} K _{2.37} Na _{0.47} Al _{8.5} Si _{27.3} O _{72.01} ·26.47H ₂ O	–42872.7 ¹¹	–43064.7	–0.45	–0.40
Ferri-mord.	Ca _{1.2} Mg _{0.48} K _{0.3} Na _{2.52} Al _{6.12} Si _{29.82} O ₇₂ ·17.34H ₂ O	–39667.8 ¹²	–39451.6	0.55	0.31
Gismondite	Ca _{0.85} K _{0.01} Na _{0.07} Al _{1.98} Si _{2.11} O _{8.08} ·4.32H ₂ O	–5541.8 ⁸	–5536.9	0.09	–0.36
Gmelinite	Ca _{0.14} Mg _{0.07} K _{0.49} Na _{7.67} Al _{8.26} Si _{15.66} O ₄₈ ·24.4H ₂ O	–31276.9 ¹³	–31324.6	–0.15	–0.14
Mord-epistil.	Ca _{0.6} K _{0.04} Na _{0.26} Al _{1.48} Si _{4.52} O _{12.01} ·3.85H ₂ O	–7027.3 ¹⁴	–7036.6	–0.13	–0.33
Stilbite	Ca _{1.01} Na _{0.12} Al _{2.12} Si _{6.88} O _{18.01} ·7.27H ₂ O	–11017.6 ¹⁵	–10953.1	0.59	0.14
Zeolite Y	Na _{0.2818} Al _{0.2818} Si _{0.71815} O _{1.9999} ·1.2765H ₂ O	–1360.1 ¹⁶	–1357.6	0.19	0.26
Zeolite A	Na _{0.5067} Al _{0.501} Si _{0.4974} O _{1.99965} ·1.0906H ₂ O	–1363.7 ¹⁶	–1373.4	–0.71	–0.41
Analcime	NaAlSi ₂ O ₆ ·H ₂ O	–3303.2 ⁶	–3312.0	–0.27	0.01
Analcime	Na _{0.96} Al _{0.96} Si _{2.04} O ₆ ·1.02H ₂ O	–3301.8 ⁶	–3305.2	–0.10	0.11
Analcime	Na _{0.95} Al _{0.95} Si _{2.05} O ₆ ·1.025H ₂ O	–3294.1 ⁶	–3303.5	–0.29	–0.09
Analcime	Na _{1.03} Al _{1.03} Si _{1.97} O ₆ ·0.985H ₂ O	–3314.9 ⁶	–3317.0	–0.07	0.25
Analcime	Na _{1.016} Al _{1.016} Si _{1.984} O ₆ ·0.992H ₂ O	–3312.3 ⁶	–3314.7	–0.07	0.23
Analcime	Na _{0.946} Al _{0.946} Si _{2.054} O ₆ ·1.027H ₂ O	–3298.7 ⁶	–3302.8	–0.13	0.06
Analcime	Na _{1.049} Al _{1.049} Si _{1.951} O ₆ ·0.976H ₂ O	–3319.5 ⁶	–3320.4	–0.03	0.33
Mean absolute value				0.30	0.25

* Diff. = [(experimental ΔH_f^0 – estimated ΔH_f^0)/experimental ΔH_f^0] × 100; ** Mathieu and Vieillard (2010); ¹ Fridriksson *et al.* (2001); ² Yang *et al.* (2001); ³ Kiseleva *et al.* (2001a); ⁴ Ogorodova *et al.* (2002a); ⁵ Kiseleva *et al.* (2001b); ⁶ Neuhoff *et al.* (2004); ⁷ Redkin and Hemley (2000); ⁸ Ogorodova *et al.* (2003); ⁹ Ogorodova *et al.* (2005); ¹⁰ Ogorodova *et al.* (2007); ¹¹ Ogorodova *et al.* (2001); ¹² Mel'chakova *et al.* (2004); ¹³ Ogorodova *et al.* (2002b); ¹⁴ Ogorodova *et al.* (2000); ¹⁵ Kiseleva *et al.* (2001b); ¹⁶ Turner *et al.* (2008).

associated with the estimation procedure is suggested by the level of disagreement between predicted and experimentally determined ΔG_f^0 and ΔH_f^0 values for minerals not included in the calibration dataset.

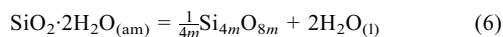
Thermodynamic interpretation of model parameters A and A*

Calorimetric investigations of the thermodynamic properties of pure-silica polymorphs having a zeolite-like structure (zeosils) have demonstrated that for all such polymorphs, including structure types MEL, MWW, IFR, ITE, AST, STT, CHA, BEA, MFI, CFI, ISV, AFI, MTW, FAU, and FER (see Passaglia and

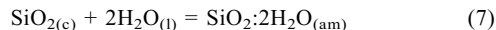
Sheppard, 2001), the enthalpy of transition from the stable oxide, α -quartz, to zeosil on a per mol SiO₂ basis is small and lies within a narrow range between 2.2 to 14.4 kJ mol⁻¹ at 298.15 K and 1 bar (Johnson *et al.*, 1987; Patarin *et al.*, 1989; Petrovic *et al.*, 1993; Navrotsky 1997; Piccione *et al.*, 2000; Moloy *et al.*, 2002). All known zeosils are thus only slightly metastable with respect to quartz, and, although the extent of metastability can be correlated empirically with changes in framework density (defined as the number of tetrahedral cations per 1000 Å³), variations in features related to framework topology, including non-bonded Si–Si distances, number of rings, or differences

in loop configurations, do not significantly affect the energetics of the quartz to zeosil transition (Petrovic *et al.*, 1993; Piccione *et al.*, 2000). Navrotsky (1997) noted that the enthalpy of transition from quartz to zeosil tends to level off with increasing molar volume, reaching a maximum value of ~ 15 kJ mol⁻¹ for zeosils of the faujasite (FAU) structure type.

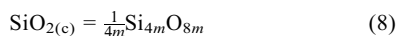
These observations are consistent with the approximations $A = A^* = 0$ kJ mol⁻¹ adopted in the present study. These parameters can be interpreted to represent ΔG_r^0 and ΔH_r^0 , respectively, for the reaction:



where the amorphous hydrous oxide is taken to represent model component Si(OH)₄, and Si_{4m}O_{8m} represents a pure-silica zeolite framework, *i.e.* a zeosil. The corresponding reaction for formation of the framework from α -quartz [SiO_{2(c)}] can be derived by adding the reaction



to reaction 6, resulting in



Assuming the Gibbs free energy change for reaction (6) [$\Delta G_{r(6)}^0$] = $A = 0$ kJ mol⁻¹, then $\Delta G_{r(8)}^0 = \Delta G_{r(7)}^0$, which implies that all zeosils should be as metastable with respect to α -quartz as is SiO₂·2H₂O_(am) on a per mol SiO₂ basis. This observation is qualitatively consistent with the experimental results noted above, indicating that all known zeosils are only slightly metastable with respect to quartz. Similarly, using ΔH_r^0 for SiO₂·2H₂O_(am) and H₂O_(l) (Table 2) and $\Delta H_r^0 = -910.700$ kJ mol⁻¹ for α -quartz (Richet *et al.*, 1982), $\Delta H_{r(7)}^0$ was calculated to be 6.1 kJ mol⁻¹ at 298.15 K. This value is equal to that of $\Delta H_{r(8)}^0$, assuming $\Delta H_{r(6)}^0 = A^* = 0$ kJ mol⁻¹, and is well within the narrow range of all known calorimetric enthalpies of transition from α -quartz to a zeosil on a per mol SiO₂ basis.

The consistency of the approximations $A = A^* = 0$ kJ mol⁻¹ with calorimetric data characterizing the energetics of zeosil formation from quartz suggests that the accuracy of the polymer model can be attributed to the fact that although the model does not account for important features of zeolite crystallography, including framework density and topology, the contributions of such features to ΔG_r^0 and ΔH_r^0 are negligible compared to contributions arising from the summation of ΔG_r^0 or ΔH_r^0 values for hydroxide components and contributions arising from changes in the coordination of extra-framework cations between the components and zeolite. In addition to being consistent with the available calorimetric data, the approximations $A = A^* = 0$ kJ mol⁻¹ are also convenient from a practical point of view because they obviate the need to normalize zeolite compositions, *e.g.* to a fixed number of O atoms in the unit cell.

Comparisons with alternative models

Mathieu and Vieillard (2010) developed a predictive model for the enthalpies of formation of anhydrous zeolites based on differences in electronegativity between framework and extra-framework sites, and on empirical observations relating framework density to the ΔH_r^0 of zeosils. For a constant framework type, the ΔH_r^0 for an anhydrous zeolite from oxide components is given by the sum of the products of the molar fraction of an O atom bound between any two cations multiplied by the electronegativity difference between any two consecutive cations located in extra-framework and tetrahedral sites. Estimates of ΔH_r^0 for the corresponding hydrous zeolites can then be determined using a complementary model for hydration enthalpies (Vieillard and Mathieu, 2009). Mathieu and Vieillard (2010) have shown that ΔH_r^0 values estimated using this electronegativity-based approach are more closely consistent with calorimetric values than those estimated using the polyhedral model of Chermak and Rimstidt (1989).

The polymer model gives ΔH_r^0 estimates for hydrated zeolites that are of comparable accuracy to those that can be estimated using the models of Mathieu and Vieillard (2010) and Vieillard and Mathieu (2009). Among all cases where direct comparisons can be made, the mean absolute value of errors generated by the polymer model is 0.34% whereas that of the electronegativity-based models is 0.25% (Table 6). A plot of these errors suggests that they are distributed homogeneously (Figure 3). The maximum error generated by the polymer model (+1.6%, for brewsterite) is similar to that of the electronegativity models (+1.5%, for pollucite; Mathieu and Vieillard, 2010).

This comparable accuracy between the polymer model and electronegativity-based models is of interest because the two modeling approaches differ in their treatment of zeolite crystal chemistry. The latter models account explicitly for the effects of framework crystallography on ΔH_r^0 through the use of an empirical

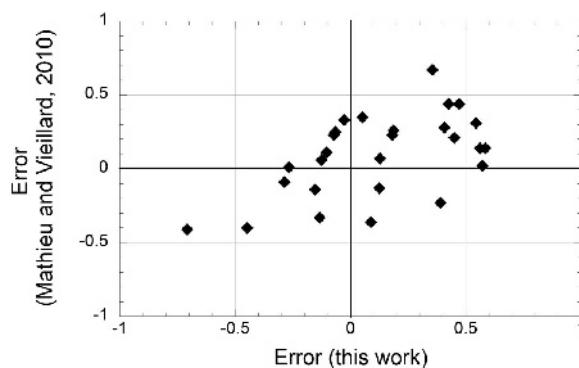


Figure 3. Comparison of errors (%) in ΔH_r^0 estimates (Table 6) using the polymer model (this study) and the electronegativity-based model of Mathieu and Vieillard (2010). Brewsterite data not shown (Table 6).

expression relating framework density, a function of unit-cell volume, to the electronegativity of Si^{4+} and Al^{3+} in tetrahedral sites of the zeolite framework relative to the electronegativity of these cations in quartz and corundum, respectively. In order to use these models, lattice parameters enabling calculation of unit-cell volumes must be known, or the volumes must themselves be estimated. In comparison, the effects of differences in the crystallography of zeolite frameworks on ΔH_f° are assumed to be negligible in the polymer model compared to contributions from the summation of ΔH_f° values for hydroxide components and the effects of changes in the coordination of extra-framework cations in the components and zeolite. The polymer model, therefore, does not require information characterizing the crystallographic properties of a zeolite's framework structure, nor separate calculations of ΔH_f° values for the anhydrous zeolite and its corresponding hydration enthalpy, and yields results that are essentially as accurate as can be obtained using the more rigorous electronegativity-based models.

The good agreement between estimated and experimental ΔG_f° values obtained using the revised polymer model ($\pm 0.2\%$) can be compared with results from other studies. Mattigod and McGrail (1999) determined an average difference of $\pm 0.28\%$ between estimated and experimental ΔG_f° values for 48 zeolites. This comparable accuracy between the original and revised models results largely from the fact that model parameter B was found to be identical in both studies within uncertainty limits. Mattigod and McGrail (1999) applied the models of Chermak and Rimstidt (1989) and La Iglesia and Aznar (1986) to the experimental dataset considered in their 1999 study and determined average differences between estimated and experimental ΔG_f° values of $\pm 0.47\%$ and $\pm 0.40\%$, respectively.

DISCUSSION

Zeolites are of interest in safety assessments of geologic repositories for nuclear wastes because they are likely to form as reaction products of water–rock–barrier interactions and could, therefore, play an important role in controlling the repository's geochemical environment. Characterizing the thermodynamic properties of these minerals is difficult, however, because their compositions tend to be variable within limits depending on the environment in which they form (Passaglia and Sheppard, 2001). The effects of this compositional variability on equilibrium properties such as the solubility can be evaluated using solid-solution models (Neuhoff *et al.*, 2004; Fridriksson *et al.*, 2001), but such models are not available for most zeolites.

An alternative approach is to approximate a zeolite's thermochemical behavior in terms of one or more fixed stoichiometric compositions that are considered to be representative or bounding with respect to certain types

of geochemical environments in which zeolites are typically found (Chipera and Apps, 2001; Savage *et al.*, 2007). This approach was evaluated by using the polymer model to estimate ΔG_f° and ΔH_f° values for zeolites in natural systems, including saline alkaline lakes and volcanoclastic rocks subjected to the effects of low-temperature diagenesis, which are believed to be similar in certain respects to environments that could evolve in a HLW repository.

The waters in alkaline lakes tend to be highly alkaline with extremely high concentrations of Na^+ and K^+ (often exceeding 100,000 ppm; Jones *et al.*, 1967) and low concentrations of Ca^{2+} due to high evaporation rates, leading to the precipitation of Ca sulfates and carbonates. Such solutions are compositionally similar to relatively young alkaline cement porewaters in which $(m_{\text{Na}^+} + m_{\text{K}^+}) > m_{\text{Ca}^{2+}}$ (Pfungsten and Shiotsuki, 1998). Volcanoclastic rocks found in alkaline lake environments alter to a mixture of zeolites, montmorillonites, feldspars, illites, and amorphous silica. Representative compositions for these zeolites, including clinoptilolite, phillipsite, chabazite, erionite, and analcime, have already been defined by Chipera and Apps (2001) (Table 7). Nominal idealized compositions were also considered in the present study for several calcic zeolites, including epistilbite, scolecite, stilbite, wairakite, and yugawaralite, which could form in a HLW repository by reactions involving older cementitious leachates that are relatively depleted in Na^+ and K^+ and enriched in Ca^{2+} (Pfungsten and Shiotsuki, 1998).

Diagenetic environments include those associated with the alteration of siliceous rocks by initially dilute, near-neutral meteoric waters, such as the altered sequences of tuffs and lavas at Yucca Mountain, Nevada. Chipera and Apps (2001) defined representative compositions for these diagenetic zeolites, which include clinoptilolite, heulandite, laumontite, mordenite, analcime, chabazite, erionite, and phillipsite (Table 7).

Assuming these compositional constraints exemplify plausible ranges in the chemistry of zeolites that could form in a HLW repository, the polymer model was used to estimate corresponding ΔG_f° and ΔH_f° values. Results indicated that in instances where direct comparisons can be made between zeolites having different compositions but with an equivalent amount of O and H_2O per formula unit (*i.e.* for chabazites, clinoptilolites, erionites, and phillipsites), differences in the ΔG_f° estimates can be as large as several hundred kJ mol^{-1} and can generate corresponding differences of up to ~ 7 log units in calculated K values for the respective dissolution reactions (Table 7). This observation is consistent with conclusions drawn from previous studies indicating that results from geochemical models of evolving conditions in a HLW repository can vary significantly depending on the compositions and thermochemical properties assumed for zeolites and other reaction products (Oda *et al.*, 2004).

Table 7. Representative compositions for zeolites in alkaline-lake (“_a”) and diagenetic (“_d”) systems (Chipera and Apps, 2001), and corresponding thermodynamic properties at 298.15 K and 1 bar estimated using the polymer model.

Zeolite	Composition	ΔG_f° (kJ mol ⁻¹)	ΔH_f° (kJ mol ⁻¹)	log K ^a
Analcime	NaAlSi ₂ O ₆ ·H ₂ O	-3096.3	-3312.0	5.5
Analcime ^b	Na _{10.2} Al _{10.2} Si _{25.8} O ₇₂ ·12H ₂ O	-36600.8	-39181.6	40.3
Chabazite_a	K _{0.9} Na _{4.9} Ca _{0.8} Al _{7.4} Si _{28.6} O ₇₂ ·36H ₂ O	-41492.3	-45240.0	-3.6
Chabazite_d	K ₂ Na _{3.7} Ca _{1.2} Al _{8.1} Si _{27.9} O ₇₂ ·36H ₂ O	-41761.4	-45510.2	3.1
Clinoptilolite_a	K _{2.3} Na _{1.7} Ca _{1.4} Al _{6.8} Si _{29.2} O ₇₂ ·26H ₂ O	-39007.1	-42265.8	-16.7
Clinoptilolite_d	K _{0.8} Na _{0.4} Ca _{2.8} Al _{6.8} Si _{29.2} O ₇₂ ·26H ₂ O	-39010.2	-42319.3	-15.5
Epistilbite	CaAl ₂ Si ₆ O ₁₆ ·5H ₂ O	-8643.8	-9354.8	3.4
Erionite_a	K _{2.8} Na _{3.4} Ca _{0.8} Al _{7.8} Si _{28.2} O ₇₂ ·30H ₂ O	-40257.7	-43695.0	-2.4
Erionite_d	K ₃ Na _{1.2} Ca ₂ Al _{8.2} Si _{27.8} O ₇₂ ·30H ₂ O	-40434.8	-43901.1	0.7
Heulandite_d	K _{0.4} NaCa _{3.3} Al ₈ Si ₂₈ O ₇₂ ·26H ₂ O	-39385.9	-42716.3	1.8
Laumontite_d	K _{0.6} Na _{0.6} Ca _{5.4} Al ₁₂ Si ₂₄ O ₇₂ ·24H ₂ O	-40233.3	-43532.0	55.3
Mordenite_d	K _{0.9} Na _{2.1} Ca _{1.5} Al ₆ Si ₃₀ O ₇₂ ·22H ₂ O	-37767.6	-40845.7	-25.0
Phillipsite_a	K _{2.8} Na _{3.2} Ca _{0.8} Al _{7.6} Si _{24.4} O ₆₄ ·24H ₂ O	-35371.8	-38299.0	6.5
Phillipsite_d	K _{1.2} Na _{1.4} Ca _{2.4} Al _{7.4} Si _{24.6} O ₆₄ ·24H ₂ O	-35317.7	-38300.4	4.7
Scolecite	CaAl ₂ Si ₃ O ₁₀ ·3H ₂ O	-5618.6	-6068.9	12.2
Stilbite	NaCa ₂ Al ₅ Si ₁₃ O ₃₆ ·14H ₂ O	-20245.2	-21973.7	15.2
Wairakite	CaAl ₂ Si ₄ O ₁₂ ·2H ₂ O	-6231.7	-6687.7	9.3
Yugawaralite	CaAl ₂ Si ₆ O ₁₆ ·4H ₂ O	-8406.6	-9068.6	3.4

^a For the balanced dissolution reaction written in terms of H⁺, Na⁺, K⁺, Ca²⁺, Al³⁺, H₄SiO₄ [as SiO_{2(aq)}], and H₂O_(l), and calculated using SUPCRT (Johnson *et al.*, 1992b), ΔG_f° for the zeolites indicated, and thermodynamic properties for aqueous species from JAEA TDB 990900 (Arthur *et al.*, 1999).

^b Applicable to both alkaline-lake and diagenetic environments (Chipera and Apps, 2001).

Uncertainties in thermodynamic properties that are attributable to the variable chemistry of zeolites can be considered in relation to uncertainties associated with techniques used to estimate these properties. Although the latter uncertainties are difficult to quantify for reasons discussed above, differences determined in the present study between experimentally determined ΔG_f° values and their estimated counterparts averaged about $\pm 0.2\%$. If this is taken as a first approximation of the total uncertainty in estimated values, zeolites with ΔG_f° values of $\sim 40,000$ kJ mol⁻¹ would have associated uncertainties of $\sim \pm 80$ kJ mol⁻¹. Such uncertainty is of similar order to differences in ΔG_f° resulting from the bounding compositions assumed for chabazites, clinoptilolites, erionites, and phillipsites (Table 7). Uncertainties related to both the inherent compositional variability of these minerals and empirical methods used to estimate their thermochemical properties can thus be substantial and should be considered when modeling the evolution of the geochemical environment in a HLW repository.

When estimated properties for minerals are included in a thermodynamic database, a single empirical model should ideally be adopted in order to avoid ambiguities that can arise if multiple models are used instead in conjunction with thermodynamic properties for model components that may not be internally consistent (Chipera and Apps, 2001; Savage *et al.*, 2007). A case in point is illustrated in Figure 4, where ΔG_f° values for several zeolites estimated using the polymer model are

compared with corresponding values estimated by Chipera and Apps (2001) using the polyhedral model of Chermak and Rimstidt (1989). As can be seen, estimates using the polyhedral model are consistently more negative (by ~ 100 kJ mol⁻¹ on average) than those obtained using the polymer model, which indicates that the former model tends to systematically over predict zeolite stabilities compared to the latter. Such tendencies, or biases, may be a source of ambiguity in interpretations of the relative stabilities of zeolites if

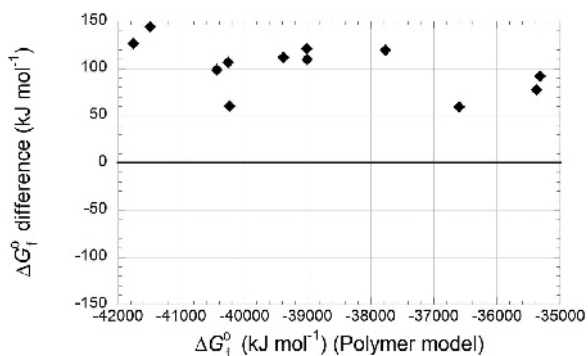


Figure 4. Plot of ΔG_f° estimated using the polymer model (abscissa) vs. the difference between these estimates and those obtained by Chipera and Apps (2001) using the polyhedral model of Chermak and Rimstidt (1989) (ordinate) for analcime, chabazite_a, chabazite_d, clinoptilolite_a, clinoptilolite_d, erionite_a, erionite_d, heulandite, laumontite, mordenite, phillipsite_a, and phillipsite_d (Table 7).

the respective ΔG_f^0 values were, for example, estimated using either the polyhedral or polymer model indiscriminately rather than just one of these models in a consistent fashion. Similar difficulties can be anticipated if ΔG_f^0 values for a group of minerals (e.g. smectites) were estimated using a technique that may not be compatible with that used for another group (e.g. zeolites).

CONCLUSIONS

Reliable interpretations of the relative thermochemical stabilities of zeolites and closely associated phases can be made if the interpretations are supported by an accurate and internally consistent set of standard thermodynamic properties for all relevant minerals, aqueous species, gases, and reactions. The present study developed a revised polymer model that can be used to estimate ΔG_f^0 and ΔH_f^0 values for zeolites, and strengthened the conceptual basis of the original model by evaluating experimental and thermodynamic constraints on adjustable model parameters. Model accuracy was determined to be comparable to, or better than, that of alternative models. A distinct advantage of the polymer approach is that it can be applied to zeolites, clay minerals, and possibly other minerals in the CASH system using a common set of calorimetrically determined thermodynamic properties for model components. This affords the development of an internally consistent set of estimated ΔG_f^0 and ΔH_f^0 values for these minerals, which in the absence of relevant experimental data can serve as a basis for interpreting their relative thermochemical stabilities as a function of temperature and aqueous ionic activities and activity ratios.

ACKNOWLEDGMENTS

The authors thank C. Oda and A. Honda of JAEA for their insightful comments and suggestions. This study was part of a broader investigation ("Project for Grouting Technology Development for a Radioactive Waste Repository") funded by the Japanese Ministry of Economics, Trade and Industry (METI). The authors thank J. Stucki and three anonymous reviewers for constructive comments on a previous version of this manuscript.

REFERENCES

Armbruster, T. and Gunter, M.E. (2001) Crystal structure of natural zeolites. Pp. 1–67 in: *Natural Zeolites: Occurrence, Properties, Applications* (D.L. Bish and D.W. Ming, editors). Reviews in Mineralogy and Geochemistry, **45**. Mineralogical Society of America, Washington D.C. and the Geochemical Society, St. Louis, Missouri, USA.

Arthur, R.C., Sasamoto, H., Shibata, M., Yui, M., and Neyama, A. (1999) Development of thermodynamic databases for geochemical calculations. JNC TN8400 99-079, Japan Nuclear Cycle Development Institute, Tokai-mura, Ibaraki, Japan.

Benning, L.G., Wilkin, R.T., and Barnes, H.L. (2000) Solubility and stability of zeolites in aqueous solution: II. Calcic clinoptilolite and mordenite. *American Mineralogist*, **85**, 495–508.

Chen, C.H. (1975) A method of estimation of standard free energies of formation of silicate minerals at 298.15°K. *American Journal of Science*, **275**, 801–817.

Chermak, J.A. and Rimstidt, J.D. (1989) Estimating the thermodynamic properties (ΔG_f^0 and ΔH_f^0) of silicate minerals at 298 K from the sum of polyhedral contributions. *American Mineralogist*, **74**, 1023–1031.

Chipera, S.J. and Apps, J.A. (2001) Geochemical stability of natural zeolites. Pp. 117–161 in: *Natural Zeolites: Occurrence, Properties, Applications* (D.L. Bish and D.W. Ming, editors). Reviews in Mineralogy and Geochemistry, **45**. Mineralogical Society of America, Washington D.C. and the Geochemical Society, St. Louis, Missouri, USA.

Cho, M., Maruyama, S., and Liou, J.G. (1987) An experimental investigation of heulandite-laumontite equilibrium at 1000 to 2000 bar P_{fluid} . *Contributions to Mineralogy and Petrology*, **97**, 43–50.

Donahoe, R.J., Liou, J.G., and Hemingway, B.S. (1990a) Thermochemical data for merlinoite: 2. Free energies of formation at 298.15 K of six synthetic samples having various Si/Al and Na/(Na + K) ratios and application to saline, alkaline lakes. *American Mineralogist*, **75**, 201–208.

Donahoe, R.J., Hemingway, B.S., and Liou, J.G. (1990b) Thermochemical data for merlinoite: 1. Low-temperature heat capacities, entropies, and enthalpies of formation at 298.15 K of six synthetic samples having various Si/Al and Na/(Na + K) ratios. *American Mineralogist*, **75**, 188–200.

Fridriksson, T., Neuhoff, P.S., Arnórsson, S., and Bird, D.K. (2001) Geological constraints on the thermodynamic properties of the stilbite-stellerite solid solution in low-grade metabasalts. *Geochimica et Cosmochimica Acta*, **65**, 3993–4008.

Gunnarsson, I. and Arnórsson, S. (2000) Amorphous silica solubility and the thermodynamic properties of $H_4SiO_4^0$ in the range of 0° to 350°C at P_{sat} . *Geochimica et Cosmochimica Acta*, **64**, 2295–2307.

Helgeson, H.C., Delany, J.M., Nesbitt, H.W., and Bird, D.K. (1978) Summary and critique of the thermodynamic properties of rock-forming minerals. *American Journal of Science*, **278-A**, 1–229.

Howell, D.A., Johnson, G.K., Tasker, I.R., O'Hare, P.A.G., and Wise, W.S. (1990) Thermodynamic properties of the zeolite stilbite. *Zeolites*, **10**, 525–531.

Johnson, G.K., Flotow, H.E., O'Hare, P.A.G., and Wise, W.S. (1982) Thermodynamic studies of zeolites: analcime and dehydrated analcime. *American Mineralogist*, **67**, 736–748.

Johnson, G.K., Flotow, H.E., O'Hare, P.A.G., and Wise, W.S. (1983) Thermodynamic studies of zeolites: natrolite, mesolite, and scolecite. *American Mineralogist*, **68**, 1134–1145.

Johnson, G.K., Flotow, H.E., O'Hare, P.A.G., and Wise, W.S. (1985) Thermodynamic studies of zeolites: heulandite. *American Mineralogist*, **70**, 1065–1071.

Johnson, G.K., Tasker, I.R., Howell, D.A., and Smith, J.V. (1987) Thermodynamic properties of silicalite SiO_2 . *Journal of Chemical Thermodynamics*, **19**, 617–632.

Johnson, G.K., Tasker, I.R., Flotow, H.E., O'Hare, P.A.G., and Wise, W.S. (1992a) Thermodynamic studies of mordenite, dehydrated mordenite, and gibbsite. *American Mineralogist*, **77**, 85–93.

Johnson, J.W., Oelkers, E.H., and Helgeson, H.C. (1992b) SUPCRT92: A software package for calculating the standard molal thermodynamic properties of minerals, gases, aqueous species and reactions from 1 to 5000 bars and 0°C to 1000°C. *Computers and Geosciences*, **18**, 899–947.

Jones, B.F., Rettig, S.L., and Eugster, H.P. (1967) Silica in alkaline brines. *Science*, **158**, 1310–1314.

Kiseleva, I., Navrotsky, A., Belitsky, I.A., and Fursenko, B.A. (1996a) Thermochemistry and phase equilibria in calcium

- zeolites. *American Mineralogist*, **81**, 658–667.
- Kiseleva, I., Navrotsky, A., Belitsky, I.A., and Fursenko, B.A. (1996b) Thermochemistry of natural potassium sodium calcium leonhardite and its cation-exchanged forms. *American Mineralogist*, **81**, 668–675.
- Kiseleva, I.A., Ogorodova, L.P., Mel'chakova, L.V., Belitsky, I.A., and Fursenko, B.A. (1997) Thermochemical investigation of natural fibrous zeolites. *European Journal of Mineralogy*, **9**, 327–332.
- Kiseleva, I.A., Ogorodova, L.P., Mel'chakova, L.V., Belitskii, I.A., and Fursenko, B.A. (1998) Thermodynamic characteristics of thomsonite and edingtonite. *Vestnik Moskovskogo Universiteta Seria 4 Geologija*, **3**, 27–32.
- Kiseleva, I., Navrotsky, A., Belitsky, I., and Fursenko, B. (2001a) Thermochemical study of calcium zeolites – heulandite and stilbite. *American Mineralogist*, **86**, 448–455.
- Kiseleva, I.A., Navrotsky, A., Belitsky, I.A., and Fursenko, B.A. (2001b) Thermodynamic properties of the calcium zeolites stilbite and stellerite. *Geochemistry International*, **39**, 170–176.
- La Iglesia, A. and Aznar, A.J. (1986) A method of estimating the Gibbs energies of formation of zeolites. *Zeolites*, **6**, 26–29.
- Mathieu, R. and Vieillard, P. (2010) A predictive model for the enthalpies of formation of zeolites. *Microporous and Mesoporous Materials*, **132**, 335–351.
- Mattigod, S.V. and McGrail, B.P. (1999) Estimating the standard free energy of formation of zeolites using the polymer model. *Microporous and Mesoporous Materials*, **27**, 41–47.
- Mattigod, S.V. and Sposito, G. (1978) Improved method for estimating the standard free energies of formation ($\Delta G_{f,298.15}$) of smectites. *Geochimica et Cosmochimica Acta*, **42**, 1753–1762.
- Mel'chakova, L.V., Ogorodova, L.P., Kiseleva, I.A., Belitskii, I.A., and Fursenko, B.A. (1999) Thermochemical investigations of natural bikitaite. *Geochemistry International*, **37**, 1224–1227.
- Mel'chakova, L.V., Ogorodova, L.P., Kiseleva, I.A., and Belitskii, I.A. (2004) Thermodynamic properties of ferrierite-mordenite-group natural zeolite. *Zhurnal Fizicheskoi Khimii*, **78**, 2300–2301.
- Moloy, E.C., Davila, L.P., Shackelford, J.F., and Navrotsky, A. (2002) High-silica zeolites: a relationship between energetics and internal surface area. *Microporous and Mesoporous Materials*, **54**, 1–13.
- Murphy, W.M., Pabalan, R.T., Prikryl, J.D., and Goulet, C.J. (1996) Reaction kinetics and thermodynamics of aqueous dissolution and growth of analcime and Na-clinoptilolite at 25°C. *American Journal of Science*, **296**, 128–186.
- Navrotsky, A. (1997) Issues in the energetics of metastable oxides and oxyhydroxides. Pp. 3–14 in: *Aqueous Chemistry and Geochemistry of Oxides, Oxyhydroxides and Related Materials* (J.A. Voigt, T.E. Wood, B.C. Bunker, W.H. Casey, and L.J. Crossey, editors). Materials Research Society Symposium Proceedings, **432**, Pittsburgh, Pennsylvania, USA.
- Neuhoff, P.S., Hovis, G.L., Balassone, G., and Stebbins, J.F. (2004) Thermodynamic properties of analcime solid solutions. *American Journal of Science*, **304**, 21–66.
- Nordstrom, D.L., Plummer, L.N., Langmuir, D., Busenberg, E., May, H.M., Jones, B.F., and Parkhurst, D.L. (1990) Revised chemical equilibrium data for major water-mineral reactions and their limitations. Pp. 398–413 in: *Chemical Modeling of Aqueous Systems II* (D.C. Melchior and R.L. Bassett, editors). ACS Symposium Series **416**, American Chemical Society, Washington D.C.
- Nriagu, J.O. (1975) Thermochemical approximations for clay minerals. *American Mineralogist*, **60**, 834–839.
- Oda, C., Honda, A., and Savage, D. (2004) An analysis of cement-bentonite interaction and evolution of pore water chemistry. Pp 73–79 in: *Proceedings of the International Workshop on Bentonite-Cement Interactions in Repository Environments* (R. Metcalfe and C. Walker, editors). NUMO-TR-04-05, Nuclear Waste Management Organization of Japan, Tokyo.
- Ogorodova, L.P., Kiseleva, I.A., Mel'chakova, L.V., Belitskii, I.A., and Fursenko, B. (1996) Enthalpies of formation and dehydration of natural analcime. *Geochemistry International*, **34**, 980–984.
- Ogorodova, L.P., Mel'chakova, L.V., Kiseleva, I.A., Belitskii, I.A., and Fursenko, B.A. (2000) Thermodynamic characteristics of mordenite group zeolite: epistilbite. *Vestnik Moskovskogo Universiteta Seria 4 Geologija*, **55**, 61–64.
- Ogorodova, L.P., Mel'chakova, L.V., Kiseleva, I.A., and Belitskii, I.A. (2001) Thermodynamic properties of natural erionite from calorimetric data. *Vestnik Moskovskogo Universiteta Seria 4 Geologija*, **56**, 56–59.
- Ogorodova, L.P., Kiseleva, I.A., Mel'chakova, L.V., and Belitskii, I.A. (2002a) Thermodynamic properties of calcium and potassium chabazites. *Geochemistry International*, **40**, 466–471.
- Ogorodova, L.P., Mel'chakova, L.V., Kiseleva, I.A., and Belitskii, I.A. (2002b) Calorimetric investigation of the natural gmelinite. *Vestnik Moskovskogo Universiteta Seria 4 Geologija*, **57**, 71–73.
- Ogorodova, L.P., Mel'chakova, L., Kiseleva, I.A. and Belitskii, I.A. (2003) Thermodynamic properties of natural zeolites of the gismondine–harronite group. *Russian Journal of Physical Chemistry*, **77**, 1543–1545.
- Ogorodova, L.P., Mel'chakova, L.V., Kiseleva, I.A., and Belitskii, I.A. (2005) Thermodynamic characteristics of natural brewsterite. *Geochemistry International*, **43**, 721–723.
- Ogorodova, L.P., Mel'chakova, L.V., and Kiseleva, I.A. (2007) A study of dachiardite, a natural zeolite of the mordenite group. *Russian Journal of Physical Chemistry*, **81**, 1748–1750.
- Passaglia, E. and Sheppard, R.A. (2001) The crystal chemistry of zeolites. Pp. 69–116 in: *Natural Zeolites: Occurrence, Properties, Applications* (D.L. Bish and D.W. Ming, editors). Reviews in Mineralogy and Geochemistry, **45**. Mineralogical Society of America, Washington D.C. and the Geochemical Society, St. Louis, Missouri, USA.
- Patarin, J., Soulard, M., Kessler, H., Guth, J.L., and Diot, M. (1989) Enthalpies standard de formation d'échantillons zéolithiques de type MFI. Stabilisation de cette structure par les cations tetra-, tri at dipropylammonium. *Thermochimica Acta*, **146**, 21–38.
- Petrova, N. (1997) Enthalpy of formation of chabazite, heulandite and clinoptilolite. *Comptes rendus de l'Académie Bulgare des Sciences*, **50**, 69–72.
- Petrovic, I., Navrotsky, A., Davis, M.E., and Zones, S.I. (1993) Thermochemical study of the stability of frameworks in high silica zeolites. *Chemistry of Materials*, **5**, 1805–1813.
- Piccione, P.M., Laberty, C., Yang, S., Camblor, M.A., Navrotsky, A., and Davis, M.E. (2000) Thermochemistry of pure-silica zeolites. *Journal of Physical Chemistry B*, **104**, 10001–10011.
- Pfingsten, W. and Shiotsuki, M. (1998) Modeling a cement degradation experiment by a hydraulic transport and chemical equilibrium coupled code. Pp. 805–812 in: *Scientific Basis for Nuclear Waste Management XXI* (I.G. McKinley and C. McCombie, editors). Materials Research Society Symposium Proceedings, **506**. Materials Research Society, Warrendale, Pennsylvania, USA.
- Redkin, A.F. and Hemley, J.J. (2000) Experimental Cs and Sr

- sorption on analcime in rock-buffered systems at 250–300°C and P_{sat} and the thermodynamic evaluation of mineral solubilities and phase relations. *European Journal of Mineralogy*, **12**, 999–1014.
- Richet, P., Bottinga, Y., Denielou, L., Petit, J., and Tequi, C. (1982) Thermodynamic properties of quartz, cristobalite and amorphous SiO_2 : Drop calorimetry measurements between 1000 and 1800 K and a review from 0–2000 K. *Geochimica et Cosmochimica Acta*, **46**, 2639–2658.
- Rimstidt, J.D. (1997) Quartz solubility at low temperatures. *Geochimica et Cosmochimica Acta*, **61**, 2553–2558.
- Robie, R.A., Hemingway, B.S., and Fisher, J.R. (1978) Thermodynamic properties of minerals and related substances at 298.15 K and 1 bar pressure and at higher temperatures. *U.S. Geological Survey Bulletin*, **1452**.
- Savage, D., Noy, D., and Mihara, M. (2002) Modeling the interaction of bentonite with hyperalkaline fluids. *Applied Geochemistry*, **17**, 207–223.
- Savage, D., Walker, C., Arthur, R., Rochelle, C., Oda, C., and Takase, H. (2007) Alteration of bentonite by hyperalkaline fluids: A review of the role of secondary minerals. *Physics and Chemistry of the Earth*, **32**, 287–297.
- Shim, S.-H., Navrotsky, A., Gaffney, T.R., and MacDougall, J.E. (1999) Chabazite: Energetics of hydration, enthalpy of formation, and effect of cations on stability. *American Mineralogist*, **84**, 1870–1882.
- Shannon, R.D. (1976) Revised effective ionic radii and systematic studies of interatomic distances in halides and chalcogenides. *Acta Crystallographica Section A*, **32**, 751–767.
- SKB (2011) Long-term safety for the final repository for spent nuclear fuel at Forsmark. SKB TR-11-01, Swedish Nuclear Fuel and Waste Management Co., Stockholm, Sweden.
- Slaughter, M. (1966) Chemical binding in silicate minerals – II. Computational methods and approximations for the binding energy of complex silicates. *Geochimica et Cosmochimica Acta*, **30**, 315–322.
- Sposito, G. (1985) Chemical models of weathering in soils. Pp. 1–18 in: *Chemistry of Weathering* (J.I. Drever and D. Reidel, editors). Dordrecht, The Netherlands.
- Sposito, G. (1986) The polymer model of thermochemical clay mineral stability. *Clays and Clay Minerals*, **34**, 198–203.
- Stull, D.R. and Prophet, H. (1971) JANAF Thermochemical Tables. NSRDS-NBS 37, U.S. Department of Commerce, National Bureau of Standards, Washington D.C.
- Tardy, Y. and Garrels, R.M. (1974) A method of estimating the Gibbs energies of formation of layer silicates. *Geochimica et Cosmochimica Acta*, **38**, 1101–1116.
- Tardy, Y. and Garrels, R.M. (1976) Prediction of Gibbs energies of formation – I. Relationships among Gibbs energies of formation of hydroxides, oxides and aqueous ions. *Geochimica et Cosmochimica Acta*, **40**, 1051–1056.
- Turner, S., Sieber, J.R., Vetter, T.W., Zeisler, R., Marlow, A.F., Moreno-Ramirez, M.G., Davis, M.E., Kennedy, G.J., Borghard, W.G., Yang, S., Navrotsky, A., Toby, B.H., Kelly, J.F., Fletcher, R.A., Windsor, E.S., Verkouteren, J.R., and Leigh, S.D. (2008) Characterization of chemical properties, unit cell parameters and particle size distribution of three zeolite reference materials: RM 8850 – zeolite Y, RM 8851 – zeolite A and RM 8852 – ammonium ZSM-5 zeolite. *Microporous and Mesoporous Materials*, **107**, 252–267.
- Vieillard, P. (2010) A predictive model for the entropies and heat capacities of zeolites. *European Journal of Mineralogy*, **22**, 823–836.
- Vieillard, P. and Mathieu, R. (2009) A predictive model for the enthalpies of hydration of zeolites. *American Mineralogist*, **94**, 565–577.
- Wagman, D.D., Evans, W.H., Parker, V.B., Schumm, R.H., Halow, I., Bailey, S.M., Churney, K.L., and Nuttal, R. L. (1982) The NBS tables of chemical thermodynamic properties. *Journal of Physical and Chemical Reference Data*, **11**, Supplement no. 2.
- Wilkin, R.T. and Barnes, H.L. (1998) Solubility and stability of zeolites in aqueous solution: I. Analcime, Na-, and K-clinoptilolite. *American Mineralogist*, **83**, 746–761.
- Yang, S., Navrotsky, A., and Wilkin, R. (2001) Thermodynamics of ion-exchanged and natural clinoptilolite. *American Mineralogist*, **86**, 438–447.
- Yui, M., Azuma, J., and Shibata, M. (1999) JNC thermodynamic database for performance assessment of high-level radioactive wastes disposal system. JNC TN8400 99-070, Japan Nuclear Cycle Development Institute, Tokai-mura, Japan.
- Yui, M., Sasamoto, H., and Arthur, R. (2004) Geostatistical and geochemical classification of groundwaters considered in safety assessment of a deep geologic repository for high-level radioactive wastes in Japan. *Geochemical Journal*, **38**, 33–42.
- Zeng, Y. and Liou, J.G. (1982) Experimental investigation of yugawaralite-wairakite equilibrium. *American Mineralogist*, **67**, 937–943.

(Received 28 October 2011; accepted 10 November 2011; Ms. 624; A.E. S. Kuznicki)